Entropy and caloric curve for mononuclei considering both surface diffuseness and self-similar expansion degrees of freedom

L. G. Sobotka[1,2] and R. J. Charity[1]
[1]*Department of Chemistry, Washington University, St. Louis, Missouri 63130, USA*
[2]*Department of Physics, Washington University, St. Louis, Missouri 63130, USA*
(Received 29 June 2005; published 25 January 2006)

The caloric curve for mononuclear configurations is studied with a model that allows for both increased surface diffusness and self-similar expansion. The evolution of the effective mass with density and excitation is included in a schematic fashion. The entropies, extracted in a local-density approximation, confirm that nuclei posess a soft mode that is predominately a surface expansion. We also find that the *mononuclear* caloric curve (temperature versus excitation energy) exhibits a plateau. Thus a plateau should be the expectation with or without a multifragmentationlike phase transition. This conclusion is relevant only for reactions that populate the mononuclear region of phase space.

DOI: 10.1103/PhysRevC.73.014609 PACS number(s): 25.70.Gh, 25.70.Pq

I. INTRODUCTION

In recent work it was shown that the mononuclear caloric curve (temperature T versus excitation energy per particle ϵ) exhibits a pseudo plateau that is due to the combined influence of expansion and in-medium effects [1,2]. This recalibration of the caloric-curve expectation, from the standard Fermi gas dependence ($T \propto \sqrt{U}$, where U is the noncollective thermal energy) to one more reminiscent of a system undergoing a first-order phase transition, is a direct consequence of the finiteness of real nuclei. This paper presents details not in our letter [2] and removes one of the significant shortcomings of our previous work by considering expansion outside the self-similar family of shapes. Specifically, we now consider both a surface-expansion degree of freedom (b) as well as an overall self-similar expansion degree of freedom (c).

Two-dimensional entropy maps $S(b, c)$ are calculated as functions of excitation energy including the effects of both the momentum- and frequency-dependent effective-mass terms (m_k and m_ω, respectively). There are two principal results. First, a ridge in the entropy maps indicates that excited nuclei have a soft expansion mode that is predominately a surface expansion. This mode would take large surface volumes of a nucleus into density regions where infinite matter is unstable with respect to clusterization. Our second finding is that the mononuclear caloric curve (constructed from the auxiliary statistical temperature) exhibits a dependence even flatter than we found with one expansion degree of freedom. Therefore one should expect the mononuclear caloric curve to exhibit not simply a pseudo plateau but a real one. This plateau is established at rather modest excitation energies (by 2 MeV per particle) well before where one usually considers the liquid-gas phase transition to occur. The mostly surface expansion, causing the flattening of the caloric curve, can be thought of a precursor to a liquid-gas phase transition. This interpretation is consistent with mesoscopic molecular transitions.

This work then presents a new benchmark for the mononuclear expectations in the region of excitation per particle below 5 MeV. It must be stressed that the physical relevance of the results presented in this work depends on the intial population of the mononuclear region of phase space. In particular this implies an absence of collective initial conditions.

II. MODEL DESCRIPTION

A. Overview

The object of this work is to present a model for the evolution of the entropy of a mononucleus with excitation energy that takes into account, in a plausible fashion, the effects of both expansion and the inevitable loss of collectivity. We are also motivated by a desire to avoid canonical thermal treatments that explicitly invoke a finite volume and a gas phase [3–5]. As our approach does not put nuclei in a box, absolute equilibrium (or absolute thermodynamic consistency) cannot be achieved. This complementary approach forces one to imagine nuclei as metastable objects for which there is some time scale of physical relevance. This time window decreases with excitation energy. Consider the nucleus studied in this work: ^{197}Au. It is unstable with respect to both fission and α-particle decay at any excitation energy. In kinetic-decay treatments of fission (into any asymmetry [6]), one needs both the entropy within the mononuclear region of phase space and the entropy of the critical configuration leading to fission. This work provides a simple scheme for calculating the former that includes what we believe are the most important physical inputs for the highest energies for which the compound nucleus is a plausible concept.

In this work, the temperature is not a thermodynamic control variable but an auxiliary parameter dictated by the rate of change of the many-body density of states. Specifically, it is the inverse of the rate of change of the maximum entropy [in our (b, c) space] $s_M \equiv \max[s(b, c)]$, with excitation energy ε that defines the temperature

$$T = 1 \Big/ \left(\frac{\partial s_M}{\partial \varepsilon} \right) . \tag{1}$$

It is the change of these statistical temperatures with excitation energy that defines our mononuclear caloric curve $T(\varepsilon)$.

As the values of s_M are the maximum values for mononuclei, we can fulfill our objective of providing a recalibration for the expectation for the mononuclear caloric curve. (One can view the subscript on the entropy as indicating both "maximal" and "mononuclear.")

To return to a point made above, the equilibrium mononuclear condition (b, c), while locally stable, is unstable with respect to α-particle emission and fission at all excitation energies and multifragmentation at high energies. The kinetics of exploring this nonmononuclear portion of phase space (i.e., of fragment, formation) is not dealt with here. Clearly the above-mentioned time window of physical relevance for the mononuclear extremum is dependent on kinetics that in turn must exhibit substantial sensitivity to the initial conditions, over which experiments have some (albeit limited) control. For example, it is likely that in heavy-ion experiments, the many-body phase space never looks like a single (equilibrated) mononucleus, while in light-ion experiments, a mononucleus "initial condition" is plausible. The kinetics is also complicated by the age-old problem of fragment (pre)formation in the low-density surface region [7]. This preformation issue is related to, but more complicated than, the cluster contribution to the free energy of infinite uniform matter [8,9]. Cluster formation in nuclei is analogous to the finite-time clusters of water molecules in macroscopic liquid and small drops [10]. The "reality" of these clusters depends on the time scale of the experimental probe.

B. Family of shapes

The density profiles $\rho_\tau(r)$ of the two isospin partners ($\tau = n, p$) are taken to be of the same functional form, scaled in proportion to their overall fraction. The native ($\epsilon = 0$ MeV) radial profiles are of the "standard" type with a Gaussian derivative:

$$\rho_n(r, b) = \frac{\rho_o}{2}\left\{1 - \mathrm{erf}\left[\frac{r - C_o(b)}{\sqrt{2}b}\right]\right\}. \tag{2}$$

The central radius C_o is defined in terms of the effective sharp radius $R_o = r_o A^{1/3}$ (with $r_o = 1.16$ fm) and the ground-state surface width $b = 1.0$ fm by use of expansion derived by Süssmann [11] and Hasse and Myers [12]. [Corrections up to $(b/R_o)^4$ were included to ensure volume conservation to high accuracy.] The expansion of nuclei with excitation is limited to the (b, c) spherically symmetric family

$$\rho(r, b, c) = c^3 \rho_n(cr, b). \tag{3}$$

For any given excitation energy, one finds the expansion parameters b and c by maximizing the entropy in the (b, c) space after deducing, the thermal energy U by subtracting the collective energy (needed for expansion) from the total excitation energy:

$$U/A = u = \varepsilon - \varepsilon_E. \tag{4}$$

Execution of this logic not only finds the metastable mononuclear expansion, but also ensures that the surface pressure is zero. This procedure is therefore logically different from the physically unreal but true equilibrium condition that one finds by placing a drop in a box and having a surrounding vapor supply a pressure. In the present work, rather than two distinct phases there is a single nonuniform Fermi drop. The problematic identification of phases is skirted.

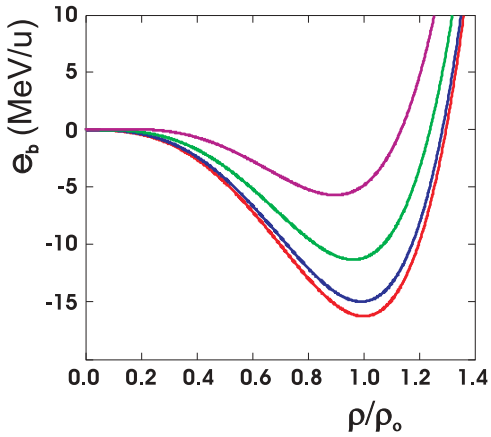

FIG. 1. (Color online) Binding energy per particle for infinite matter from [14] as a function of reduced density for asymmetries $\delta = 0.0$, 0.2, 0.4, and 0.6 (bottom to top).

C. Expansion energy

The collective energy involved in expansion is taken from a simple energy-density formalism modeled after Lombard's original work [13] but making use of a the equation of state (EOS) offered by the Thomas-Fermi (TF) model of Myers and Świątecki [14]. The energy per particle of cold uniform matter $e_b(\rho, \delta)$ is reproduced in Fig. 1 as a function of reduced density ($\bar{\rho} \equiv \rho/\rho_o$) for several asymmetries $\{\delta \equiv [(\rho_N - \rho_Z)/(\rho_N + \rho_Z)]\}$. The equilibrium density and compressibility of symmetric nuclear matter for this EOS are $\rho_o = 0.16144$ fm^{-3} and $K_o = 234$ MeV, respectively.

The binding energy ($-\varepsilon_{\mathrm{ED}}$) of a drop in the minimalist energy-density formalism used here is the sum of three terms, corresponding to (i) the binding energy of the drop, neglecting gradient corrections, what we call a "matter drop," (ii) the gradient correction term, originally introduced by van der Waals, and (iii) the Coulomb integral dealing with the fact that nuclei are one-component plasmas:

$$\varepsilon_{\mathrm{ED}}(b, c)A = \varepsilon_{\mathrm{md}}(b, c) + \varepsilon_{\mathrm{gr}}(b, c) + \varepsilon_{\mathrm{coul}}(b, c). \tag{5}$$

The terms in Eq. (5) are

$$\varepsilon_{\mathrm{md}}(b, c) = \int_0^\infty e_b(\rho, \delta)\rho(b, c, r)d\mathbf{r}, \tag{6}$$

$$\varepsilon_{\mathrm{gr}}(b, c) = \frac{\hbar^2 b_{\mathrm{gt}}}{8m}\int_0^\infty |\nabla\rho(b, c, r)|^2 d\mathbf{r}, \tag{7}$$

$$\varepsilon_{\mathrm{coul}}(b, c) = -\int_0^\infty \left(\frac{4}{3}\pi r^3 \rho_z\right)\frac{1}{r}(4\pi r^2 \rho_z dr). \tag{8}$$

The only adjustable parameter is the coefficient of the gradient term b_{gt} . The analytic Coulomb integral, assuming $\rho_Z = \rho(Z/A)$ (plus the small exchange correction) were taken from

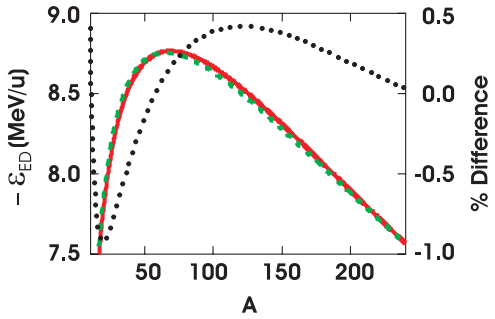

FIG. 2. (Color online) Binding energy per particle for the energy-density formalism used in this work [$\epsilon_{ED}(1, 1)$, solid curve]. Also shown are the DROPLET model binding energy per particle (dashed curve) and the percentage of difference between the DROPLET model and ϵ_{ED} (dotted curve) binding energies. The latter are referenced to the right-hand-side axis.

[12]. With a value of $b_{gt} = 14.00$, this simple energy-density formalism reproduces the binding energy of the DROPLET model [15] to within 1% (∼80 keV per particle) from $10 < A < 240$ or 0.4% if the region is limited to $50 < A < 240$; see Fig. 2. Another way to view this comparison is that this simple energy functional prescription reproduces the DROPLET model binding energies to within 1% for the leptodermous expansion parameter between $(1/7) > (b/R_o) > (1/2.5)$. In the subsequent figures, we present our results out to about $(b/R_o) \sim (1/2)$. It is the growth of the surface with excitation that limits this work to excitation energies of less than 5 MeV per particle.

Our object in introducing the simple energy-density formalism is to estimate the collective energy required for expanding to any member of the (b, c) shape family. The expansion energy [from one point in (b, c) space to another] is just the difference in binding energies. These values ε_E (per nucleon), taking the reference at (1,1) $\{\varepsilon_E = -[\varepsilon_{ED}(b, c) - \varepsilon_{ED}(1, 1)]\}$, are shown in Fig. 3 as functions of the self-similar expansion degree of freedom c for ^{197}Au. $\varepsilon_E(b = 1, c)$ has the characteristic

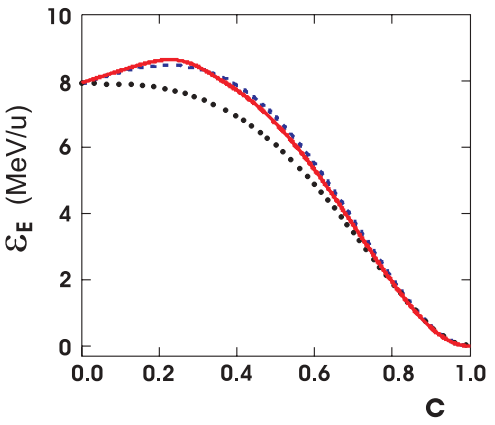

FIG. 3. (Color online) Expansion energy (per particle) as a function of the self-similar expansion degree of freedom c for the energy-density formalism used in this work (solid curve), the scaling model of Myers and Świątecki [17] (dashed curve) and the form used in EES [16] (dotted curve).

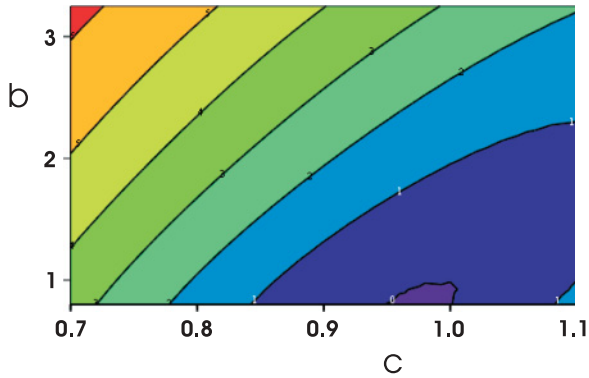

FIG. 4. (Color online) The expansion energy ε_E used in this work as a function of the both increased surface diffuseness (b) and self-similar expansion degree of freedom (c). The contours are at 1-MeV increments, starting from 0, intersecting $(b, c) = (0,0)$, and increasing from that point to the upper-left-hand corner.

inverted bell shape modeled by the simple functional form used in Friedman's EES code [16] [$\varepsilon_E^F = \varepsilon_c^F(1 - \bar{\rho})^2$, with the constant $\varepsilon_c^F \sim 8$ MeV] and is in close quantitative agreement (throughout the full range of c) with the ground-state binding-energy scaling logic of Myers and Świątecki [17] (after correction for the Coulomb energy).

Figure 4 displays $\varepsilon_E(b, c)$ (again for $A = 197$) in the physically relevant (b, c) region. Here one notes the relative softness (in terms of expansion energy) of increasing the surface diffuseness compared with the self-similar expansion. The latter requires reduction of the central density. This relative softness is well known and can be found in the Hartree-Fock results [18], also see citations in [19].

The lack of higher-order terms common in state-of-the-art energy-density models, used for example in Skyrme functionals [20,21], is not as important for the nonstructural, high-energy considerations of this work in which gradients will be *reduced* with excitation. On the other hand, both the low density and the functional form for the density profile are important issues for two different reasons. The former is physical and based on the knowledge that below $\bar{\rho} \sim 1/2$ to $1/3$, *uniform* matter is unstable with respect to clusterization [8,9]. This difficult, and perhaps intractable, physical issue we must remain cognizant of. The second issue relates to the numerical accuracy of our approach for calculating the entropy. This second issue is discussed at the end of the next section.

The question of the temperature dependence of the coefficient of the gradient term (b_{gt}) has been the focus of considerable discussion in molecular physics for a hundred years. Molecular studies indicate that any T dependence is very weak. From one point of view this is not surprising as with increasing T the relative importance of this term decreases as the surface invariably becomes more diffuse—smaller $|\nabla\bar{\rho}|$. (This term reduces the binding energy by only ∼10% for the heavy nucleus considered here at $T = 0$. The relative contribution must decrease as the surface becomes more diffuse.) However, the lack of a strong T dependence in molecular work has been justified by the following a heuristic argument [22,23]. For a planar system the dependence of b_{gt}

on the surface tension γ, isothermal compressibility κ_T, and miscibility gap $\Delta\rho$ is formally

$$b_{\rm gt} \propto \frac{\gamma^2\kappa_T}{(\Delta\rho)^4} \overset{T\to T_c}{=} \frac{\left[\left(1-\frac{T}{T_c}\right)^{1.29}\right]^2\left[\left(1-\frac{T}{T_c}\right)^{-1.25}\right]}{\left[\left(1-\frac{T}{T_c}\right)^{0.34}\right]^4}, \sim \left(1-\frac{T}{T_c}\right)^{0.03}. \quad (9)$$

The second equality gives the scaling dependence of each term, as the critical temperature T_c is approached, for classical fluids. Collecting the critical exponents, one finds that (at least for classical fluids) the temperature dependence of $b_{\rm gt}$ is expected to be exceedingly slight. The need for curvature corrections has also been investigated in the case of classical fluids [24] and found (with a suitable choice of the "surface of tension") to be negligable. In light of the above, the fact that no clear argument exists for whether $b_{\rm gt}$ should increase or decrease with T (recall that decreasing $b_{\rm gt}$ would make gradients *less* costly), and the decreasing relative importance of the term with increasing T, we have taken $b_{\rm gt}$ as independent of T.

D. Entropy

The dominant term in the expression for the entropy of a quantum drop of degenerate Fermi liquid can be written as [25]

$$S = 2\sqrt{aU} = 2\sqrt{aA(\varepsilon-\varepsilon_E)}, \quad (10)$$

where a is the level-density parameter and the total and expansion energies per nucleon are ε and ε_E, respectively.

In the local-density approximation (LDA), the level density depends on the nuclear profile, the local Fermi momentum $k_{F\tau}$, and the effective mass m_τ (for each isospin partner τ) [26,27]:

$$a = \frac{\pi^2}{4}\sum_\tau \int \frac{\rho_\tau(r)}{\left[\hbar^2 k_{F\tau}^2(r)/2m_\tau^*\right]} d\mathbf{r}. \quad (11)$$

This approximation is built on a TF logic in which the potential is removed from the problem by assuming that the relation $\rho = (1/3\pi^2)k^3$ can be used to calculate the local Fermi momentum.

We adopt the factorization of the effective mass into momentum- and frequency-dependent terms as suggested by Mahaux *et al*. [28] and Mahaux and Sartor [29], but we neglect isospin splitting. We parametrize these terms by using the phenomenological form suggested by Prakash *et al*. [27] and used by De *et al*. [30]:

$$\frac{m^*}{m} = (m_k)[m_\omega] = (1-\alpha\bar\rho(r,c))[1-\beta(T)\bar\rho'(r,c)], \quad (12)$$

with

$$\alpha = 0.3, \quad \beta(T) = 0.4A^{1/3}\exp[-(TA^{1/3}/21)^2]. \quad (13)$$

The effective-mass factor is suppressed in the bulk, peaks at the surface [31], and degrades to 1 with decreasing density or increasing thermal energy. The radial dependence of the effective mass is shown in Fig. 5. Panel a displays how the effective mass is influenced by local density and gradient and

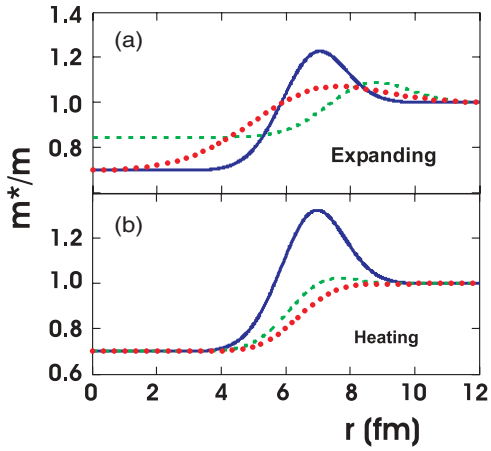

FIG. 5. (Color online) (a) Effective mass profiles for $(b, c) = (1, 1)$ (solid curve), self-similar expansion (1,0.85) (dashed curve), and increased surface diffuseness (2,1) (dotted curve). (b) Effective-mass profiles for $(b, c = (1, 1))$ and $T = 0.5$ (solid curve), 2 (dashed curve) and 4 MeV (dotted curve).

the effect of heating is shown in panel b. The primary difference between how the two expansion modes affect the effective mass is that the self-similar expansion (c) reduces the bulk density and therefore m_k/m returns to 1 (from the matter value of 0.7) in the central region while the surface degree of freedom (b) maintains the m_k/m suppression in the bulk (at least for the $A = 197$ case considered here). One should focus on the difference in m_k/m in the interior for the expansion degrees of freedom, because with heating, the surface enhancement from the m_ω term is destroyed independent of the radial profile.

The T dependence in m_ω/m requires knowing the caloric curve $[T(\varepsilon)]$. We solve this problem iteratively. A single iteration suffices to ensure that the T is uniquely determined by ε and satisfies the stationary condition. (The reason a single iteration suffices is that above $T = 2$ the $[m_\omega]$ term is returned to 1 and the collective response captured by the frequency dependence of the effective mass is played out.)

The two many-body effects, to a large extent, offset one another in near-ground-state nuclei, yielding $a \approx A/8$ for unexpanded ^{197}Au. However the destruction of the cooperativity encoded in these two effective-mass terms does not occur on identical energy scales. While the detailed density and excitation-energy dependences of these terms are unknown, the results shown below illustrate how the gross effects captured by these terms couple with expansion to dictate the form of the caloric curve.

As this work is built on the LDA, the accuracy of this approximation is a central issue. Fortunately, Shlomo has compared calculations of the level-density parameter a by using LDA, TF, TF with $\hbar^2$ corrections (SC), and Green's function techniques [32]. First he finds that the SC logic provides an excellent approximation to the (exact) quantum-mechanical Green's function results. Even TF calculations do an excellent job as long as the potential is smooth and finite. The LDA, on the other hand, overpredicts a. This overprediction is rather small for heavy nuclei (large $A^{1/3}$) and becomes progressively worse with decreasing $A^{1/3}$. The ratio

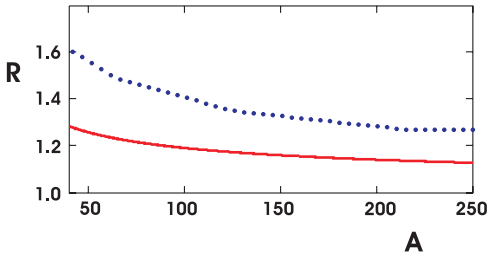

FIG. 6. (Color online) Ratio of level-density constants $a_{\mathrm{LDA-F}}/a_{\mathrm{SC-F}}$ (dotted curve) from [32] and $a_{\mathrm{LDA-F}}/a_{\mathrm{LDA-S}}$ (solid curve).

of the level density parameter, calculated with a Fermi function profile, using the LDA approximation to that calculated with the SC calculation $R = a_{\mathrm{LDA-F}}/a_{\mathrm{SC-F}}$ (from [32]) is shown in Fig. 6 as a dotted curve. The overprediction of the LDA is due to an overemphasis of the low-density surface material. This problem is amplified when the LDA is used (as Shlomo did) with the relatively long-tailed Fermi profile. Our choice of the "standard profile" is inspired by the analysis of Tõke and Świątecki [33], in which the standard profile was chosen to minimize this problem. Figure 6 also shows the level-density parameter ratio from the long-tailed Fermi function profile to the shorter-tailed standard profile, $a_{\mathrm{LDA-F}}/a_{\mathrm{LDA-S}}$, both in the LDA approximation. Use of the standard profile as opposed to a Fermi function profile removes half of the discrepancy found by Shlomo. The remaining discrepancy suggests that, to a small degree, low-density material in a LDA calculation, even with the standard profile used here, still excessively contributes to a and thus S.

III. RESULTS

The relative entropies per nucleon, $s(b, c)/s(1, 1)$ are shown in Fig. 7 for several energies. The shift in the (b, c) location of the maximum entropy with excitation energy is primarily in the b coordinate direction. This primary trend is consistent with mean-field parametrizations of the temperature dependences of the radius and surface diffuseness [18,19].

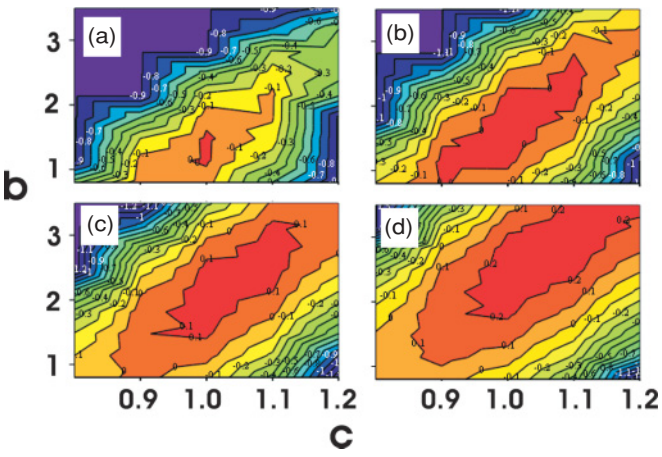

FIG. 7. (Color online) The relative entropies per nucleon $s(b, c)/s(1, 1)$ map as functions of expansion (c = abscissa) and surface diffuseness (b = ordinate) for excitation energies of $\varepsilon =$ 2, 3, 4, and 5 MeV A are shown in panels a, b, c, and d, respectively. The contours are in steps of 10%. The (unitless) absolute values of the entropy of the references states at (1,1), for each of these energies are 0.907, 1.134, 1.356, and 1.59, respectively.

Aside from the increasing surface diffuseness with excitation energy, these maps illustrate that the proper thermodynamic variable for the isolated system is a soft normal mode with both b and c characters. The positive correlation between the parameters that define the entropy ridge can be interpreted as an enhancement in the density of states when the central density is maintained at near-saturation values. Moreover, the flatness of this entropy ridge is striking. Fluctuations to very large b, with coupled increasing c, are inevitable. This is suggestive of canonical prescriptions that create a gas phase at elevated T. However, the connection is due to the inherent instability of the metastable system toward surface expansion (rather than bulk fragmentation.) This inference is related to our choice of degrees of freedom, an issue to which we return in the next section. Such a surface effect is reminiscent of well-known surface melting in mesoscopic classical systems [34].

The density profiles for the equilibrium (b, c) positions are shown in Fig. 8(a) for $\varepsilon = 2$, 3, 4, and 5 MeV. Aside from the dramatic increase in surface width with increasing excitation energy, a small increase in the central density is also observed. The shapes along the entropy ridge are shown in Fig. 8(b) for $\varepsilon = 3$ MeV. The great variation of shapes along this ridge (from those with an extremely dense core with a long tail to simply expanded shapes) is impressive. It is possible that the length of the ridge in the direction of large b and c is excessive because of the LDA approximation.

Finally, we turn to the caloric curve. We calculate $T(\varepsilon)$ by capturing the maximal entropies at a function of excitation energy and employing Eq. (1). These results, along with those for a simple Fermi gas and those if only a self-similar expansion is considered, are shown in Fig. 9. With each added expansion degree of freedom, the caloric curve becomes flatter. This provides considerable insight into the interpretation

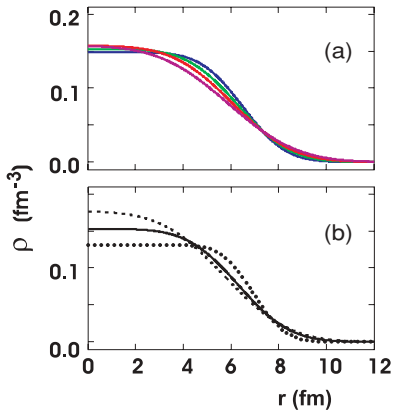

FIG. 8. (Color online) (a) Density profiles that maximizes the entropy for excitation energies of $\varepsilon = 2, 3, 4,$ and 5 MeV A. (b) Density profiles along the entropy ridge for $\varepsilon = 3$ MeV A. The solid curves represents the entropy peak while the dotted and dashed curve are extremes of the entropy ridge.

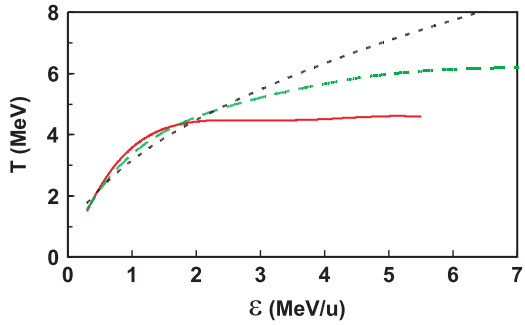

FIG. 9. (Color online) Caloric curve (for ^{197}Au) for a Fermi gas with fixed density and a level-density parameter $a = A/10$ (dotted curve), self-similar expansion (dashed curve), and both self-similar and surface expansion degrees of freedom (solid curve).

of caloric curves *for mesoscopic systems*. Such systems, as opposed to uniform infinite systems, inherently posses degrees of freedom that evolve naturally to yield a plateau. The addition of the collective surface degree of freedom is apparently sufficient to provide a representation similar to that expected in the thermodynamic limit. (This is in fact the object of thermodynamics: A few well-chosen collective variables suffice to define system observables.) However, from the metastable perspective of the present work, it is phase equilibrium and coexistence that are the auxiliary concepts. Both perspectives, metastable mononucleus with an implied time window of relevance and true phase equilibrium with unphysical boundary conditions, are of considerable heuristic value.

The general shape of the caloric curve, when two dimensions are considered, is qualitatively similar to those extracted from experimental data [35,36]. The value of the temperature plateau T_p is slightly lower than that found by Natowitz *et al.* [37], who also conclude that T_p decreases with increasing mass. The model presented in this work predicts essentially the same plateau temperature T_p for a mass 90 system as it does for a mass 197 system. While this might be considered at variance with the trend of the results of Natowitz *et al.*, we do not believe the experimental data present a compelling case for a significant dependence on mass if the data for the very lightest nuclei are excluded.

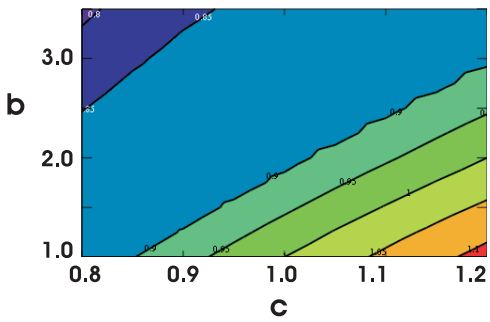

FIG. 10. (Color online) Barrier-reduction factors $k(b, c)$. The contours are at 5% increments from 1.1 to 0.80 in the lower-right-hand and upper-left-hand corners, respectively.

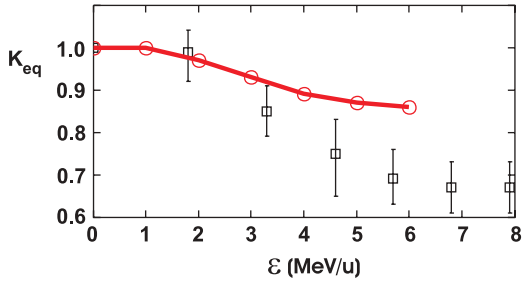

FIG. 11. (Color online) Barrier-reduction factors as functions of excitation energy per nucleon for the equilibrium shapes (circles) and those extracted from ISiS data [42] (squares with error bars.)

The equilibrium shapes can also be used to estimate the reduction in the barrier energy with excitation. The total potential and barriers B, potential extremum, were extracted from the sum of the single folded (point test particle) nuclear V_N and Coulomb V_C potential terms:

$$\begin{aligned} V_T(\mathbf{R}) &= V_N(\mathbf{R}) + V_C(\mathbf{R}), \\ &= \int \bar{\rho}(\mathbf{r}_1) V_{12}(|\mathbf{R} - \mathbf{r}_1|) d\mathbf{r}_1 \\ &\quad + \int \rho_z(\mathbf{r}_1) \left(\frac{e}{|\mathbf{R} - \mathbf{r}_1|}\right) d\mathbf{r}_1. \end{aligned} \tag{14}$$

The depth on the nuclear interaction V_{12} was taken from [38], and the range was taken to be of exponential form with a characteristic range of 0.63 fm. This range parametrization and value, when folded with the $(b, c) = (1,1)$ profile, yield a barrier height and distance in agreement with the optical-model potentials of Becchetti and Greenless [39,40] as well as of Varner *et al.* [41]. The reduction factors, $k = B(b, c)/B(1, 1)$, calculated in the relevant region of the shape parameter space, are shown in Fig. 10 while the barrier-reduction factors for the shapes along the (maximal) entropy ridge $k_{\rm eq} = B(b, c)_{\rm eq}/B(1, 1)$, extracted as functions of excitation energy, are shown in Fig. 11. The two-dimensional map shows that the reduction factors change transverse to the entropy ridge and are about constant along it. The barrier-reduction factors start at 1 at low energies, drop to between 0.90 and 0.85, and cannot, in this model, be less than 0.85 (as such values are "northeast" of the entropy ridge at even the highest energy.)

Also plotted (as squares) in Fig. 11 are the barrier-reduction factors extracted from an analysis of the fragment energy spectra in ^{3}He $+^{197}$Au bombardments [42]. The latter results, from the Indiana Silicon Sphere (ISiS), show larger reduction factors (as low as 0.7) than predicted from the equilibrium (b, c) configurations.

IV. CONCLUSIONS

The primary conclusion of this work is that a plateau in the caloric curve should be expected for a finite mononuclear system. The basic concepts of expansion and effective-mass evolution used in this this work are similar to those presented by Natowitz *et al.* [43]. This work also shares much in common with that of Chen *et al.* [44]. However, the problem is attacked

from a different perspective, and the packaging of the basic inputs in a computational scheme is different, yielding a more satisfactory heuristic presentation.

The near-constant statistical temperature is due to the energy spent on expansion and the destruction of collective effects. While this conclusion was found in our previous publication, this work not only demonstrates that the conclusion is robust with respect to explicit consideration of surface expansion, but both supports previous work, indicating the importance of the surface, and clarifies the nature of the surface-expansion mode. We find that adding degrees of freedom (dealing with the shape) allows the mesoscopic transition to appear more and more as a phase transition of a macroscopic system. We are not aware of whether this point has been made before. The importance of the surface is not at all surprising and can find its parallel in condensed matter physics, in which the study of the melting of either nanomaterials or isolated crystals becomes a study of surface melting [34].

While this work makes use of several simplifying assumptions, it is the LDA for the entropy that is most suspect. In particular, to what extent does the well-known excessive contribution from low-density material compromise our findings? While we have minimized this problem by our choice of density profile, further numerical work related to this point would be most useful. From another perspective, one can view the excessive contribution from low density in the LDA as offsetting the neglect, in this work, of the clustered contribution to the density of states. Again, additional work might be able to shed light on these, to some extent, offsetting issues.

The relevance of this work to both the concept of a limiting compound nucleus temperature [45,46] and the so-called liquid-gas phase transition [47] is profound. In addition to the plateau in the caloric curve, the observed saturation of the Giant Dipole Resonance yield [48] forces the question of when, in excitation energy, the metastability of compound nuclei gives way to instability and invalidates the concept of a Compound Nucleus [49]. The present work arrives at the same conclusion, (i.e., a limiting temperature of about 5 MeV) by a rather straightforward deduction of the caloric curve for metastable mononuclei rather than the disappearance of a solution to Gibbs' coexistence conditions. The latter represents a true equilibrium thermodynamic reality for a hypothetical (gedanken) system. Our result for a metastable mononuclei indicates that, within the time of relevance, a mononucleus has a limiting temperature, independent of phase coexistence arguments.

As far as the liquid-gas phase transition is concerned, one can certainly view the mean density reduction seen in the present model as a precursor to a phase transition (e.g., as surface melting is for the solid-liquid transition in molecular systems). However, this work highlights the subtleties of transferring phase-transition logic to the mesoscopic scale. In particular, this work suggests that the *equilibrium* path to fragmentation is by means of fragment production from low-density exterior material. New external material would again be formed at low density that would, in turn, be unstable to clusterization. While the distinction between surface and bulk is rather tenuous in medium and light nuclei, the case study of a heavy nucleus in the present work illustrates that a likely kinetic route to the deconstruction of a highly excited heavy nucleus (in the absence of collective expansion—see below) is through surface rather than bulk effects.

However, it must be appreciated that this work implicates the surface rather than more complex collective shape and density variations because the former is considered while the latter are not. The reverse is true in the work by Colonna *et al*. [50], in which multipole density fluctuations built on self-similar (scaling) expansions (i.e., our c parameter) are considered. However, it is likely that the importance of any particular mode has more to do with initial conditions than with inherent growth instabilty times [51]. One can turn this argument around. For example, one could argue that any experimental evidence for bulk disintegration or disassembly of a heavy nucleus implicates dynamical conditions seeding self-similar-type expansions. Collective radial flow would be such a condition. This work lends support to this contention in that the barrier energies are in fact lower than one calculates from metastability logic. That is, while the metastable thermodyanmic approach of the present work indicates that the expansion (and instability) is mostly surfacelike, the low fragment energies suggest real-world realizations with a more self-similar character. Nevertheless, this work serves to recalibrate expectations for the caloric curve for metastable mononuclei and illustrates the importance of the surface in the absence of dynamical initial conditions.

ACKNOWLEDGMENTS

The authors acknowledge several discussions with A. J. Sierk and J. Natowitz. This work was supported by the U.S. Department of Energy, Division of Nuclear Physics, under grant DE-FG02-87ER-40316.

[1] J. Tõke, J. Lu, and W. U. Schröder, Phys. Rev. C **67**, 034609 (2003); **67**, 044307 (2003).
[2] L. G. Sobotka, R. J. Charity, J. Tõke, and W. U. Schröder, Phys. Rev. Lett. **93**, 132702 (2004).
[3] J. N. De, S. Das Gupta, S. Shlomo, and S. K. Samaddar, Phys. Rev. C **55**, R1641 (1997).
[4] C. B. Das, S. Das Gupta, and A. Z. Mekjian, Phys. Rev. C **67**, 064607 (2003).
[5] C. B. Das, S. Das Gupta, W. G. Lynch, A. Z. Mekjian, and M. B Tsang, Phys. Rep. **406**, 1 (2005).
[6] L. G. Moretto, Nucl. Phys. **A247**, 211 (1975).
[7] D. H. Wilkinson, Comments on Nucl. Part. Phys. **1**, 36 (1967).
[8] J. W. Clark and T. P. Wang, Ann. Phys. (NY) **40**, 127 (1966).
[9] B. Friedman and V. R. Pandharipande, Nucl. Phys. **A361**, 502 (1981).

[10] D. Eisenberg and W. Kauzmann, *The Structure and Properties of Water* (Oxford University Press, New York, 1969).
[11] G. Süssmann, Z. Phys. **A274**, 145 (1975).
[12] R. W. Hasse and W. D. Myers, *Geometrical Relationships of Macroscopic Nuclear Physics* (Springer-Verlag, Berlin, 1988).
[13] R. Lombard, Ann. Phys. (NY) **77**, 380 (1973).
[14] W. D. Myers and W. J. Świątecki, Phys. Rev. C **57**, 3020 (1998).
[15] W. D. Myers, *Droplet Model of Atomic Nuclei* (IFN/Plenum Data Co., New York, 1977).
[16] W. A. Friedman, Phys. Rev. Lett. **60**, 2125 (1988).
[17] W. D. Myers and W. J. Świątecki, Nucl. Phys. **A587**, 92 (1995).
[18] M. A. Hasan and J. P. Vary, Phys. Rev. C **58**, 2754 (1998).
[19] S. Shlomo and V. M. Kolomietz, Rep. Prog. Phys. **67**, 1 (2004), and references cited therein.
[20] J. Bartel, M. Brack, and M. Durand, Nucl. Phys. **A445**, 263 (1985).
[21] P. Gleissel, M. Brack, J. Meyer, and P. Quentin, Ann. Phys. (NY) **197**, 205 (1990).
[22] S. Fisk and B. Widom, J. Chem. Phys. **50**, 3219 (1969).
[23] J. S. Rowlinson and B. Widom, *Molecular Theory of Capillarity* (Clarendon, Oxford, 1982).
[24] R. Lovett and M. Baus, Adv. Chem. Phys. **102**, 1 (1997).
[25] H. A. Bethe, Phys. Rev. **50**, 332 (1936).
[26] M. Barranco and J. Treiner, Nucl. Phys. **A351**, 269 (1981).
[27] M. Prakash, J. Wambach, and Z. Y. Ma, Phys. Lett. **B128**, 141 (1983).
[28] C. Mahaux, P. F. Bortignon, R. A. Broglia, and C. H. Dasso, Phys. Rep. **120**, 1 (1985).
[29] C. Mahaux and R. Sartor, Adv. Nucl. Phys. **20**, 1 (1991).
[30] J. N. De, S. Shlomo, and S. K. Samaddar, Phys. Rev. C **57**, 1398 (1998).
[31] R. W. Hasse and P. Schuck, Phys. Lett. **B179**, 313 (1986).
[32] S. Shlomo, Nucl. Phys. **A539**, 17 (1992).
[33] J. Tõke and W. J. Świątecki, Nucl. Phys. **A372**, 141 (1981), see appendix for discussion on profile.
[34] While there are many related references, two we have found pertinent are: Surface Properties, Adv. Chem. Phys. **105** (1996) and L. Gelb, *Theoretical Studies of Surface Phase Transitions*, Lev Gelb, Ph.D. thesis, University Of Cambridge (1995).
[35] R. Wada, D. Fabris, K. Hagel, G. Nebbia, Y. Lou, M. Gonin, J. B. Natowitz, R. Billerey, B. Cheynis, A. Demeyer, D. Drain, D. Guinet, C. Pastor, L. Vagneron, K. Zaid, J. Alarja, A. Giorni, D. Heuer, C. Morand, B. Viano, C. Mazur, C. Ngô, S. Leray, R. Lucas, M. Ribrag, and E. Tomasi, Phys. Rev. C **39**, 497 (1989).
[36] J. Pochodzalla *et al*., Phys. Rev. Lett. **75**, 1040 (1995).
[37] J. B. Natowitz, R. Wada, K. Hagel, T. Keutgen, M. Murray, A. Makeev, L. Qin, P. Smith, and C. Hamilton, Phys. Rev. C **65**, 034618 (2002).
[38] P. Möller, J. R. Nix, W. D. Myers, and W. J. Świątecki, At. Data Nucl. Data Tables **59**, 185 (1995).
[39] F. D. Becchetti Jr. and G. W. Greenless, Phys. Rev. **182**, 1190 (1969).
[40] C. M. Perey and F. G. Perey, At. Data Nucl. Data Tables **17**, 1 (1976).
[41] R. L. Varner, W. J. Thompson, T. L. McAbee, E. J. Ludwig, and T. B. Clegg, Phys. Rep. **201**, 57 (1991).
[42] D. S. Bracken, K. Kwiatkowski, E. Renshaw Foxford, K. B. Morley, V. E. Viola, N. R. Yoder, J. Brzychczyk, E. C. Pollacco, R. Legrain, C. Volant, R. G. Korteling, and H. Breuer, Phys. Rev. C **69**, 034612 (2004).
[43] J. B. Natowitz, K. Hagel, Y. Ma, M. Murray, L. Qin, S. Shlomo, R. Wada, and J. Wang, Phys. Rev. C **66**, 031601(R) (2002).
[44] X. S. Chen, C. Ngô, E. Tomasi, M. Barranco, X. Vinas, and H. Ngô, Nucl. Phys. **A401**, 143 (1983).
[45] S. Levit and P. Bonche, Nucl. Phys. **A437**, 426 (1985).
[46] H. R. Jaqaman, Phys. Rev. C **39**, 169 (1989).
[47] M. D'Agostino, R. Bougault, F. Gramegna, I. Iori, N. LeNeindre, G. V. Margagliotti, A. Moroni, and G. Vannini, Nucl. Phys. **A699**, 795 (2002).
[48] K. Yoshida, J. Kasagi, H. Hama, M. Sakurai, M. Kodama, K. Furutaka, K. Ieki, W. Galster, T. Kubo, and M. Ishihara, Phys. Lett. **B245**, 7 (1990).
[49] P. F. Bortignon, A. Bracco, D. Brink, and R. A. Broglia, Phys. Rev. Lett. **67**, 3360 (1991).
[50] M. Colonna, Ph. Chomaz, and S. Ayik, Phys. Rev. Lett. **88**, 122701 (2002).
[51] Ph. Chomaz, M. Colonna, and J. Randrup, Phys. Rep. **389**, 263 (2004).